Contribution from the Institut für Physikalische und Theoretische Chemie, Universität Tübingen, 7400 Tübingen, West Germany, and Institut für Anorganische Chemie, Universität Dortmund, 4600 Dortmund, West Germany

The Chlorofluorophosphoranes PCl_nF_{5-n} (n = 1–4). Gas-Phase Structures and Vibrational Analyses

C. Macho,[1b] R. Minkwitz,*[1b] J. Rohmann,[1b] B. Steger,[1a] V. Wölfel,[1b] and H. Oberhammer*[1a]

Received February 12, 1986

The geometric structures of the mixed chlorofluorophosphoranes PCl_nF_{5-n} with n = 1–4 have been determined by gas electron diffraction. P–F and P–Cl bonds lengthen with increasing F/Cl substitution, whereby in general axial bonds are more strongly affected. Angular distortions from the ideal trigonal bipyramid are small, less than 1° for equatorial–axial angles and about 2° for equatorial–equatorial angles. Normal-coordinate analyses for the title compounds based on matrix infrared spectra and Raman polarization measurements (liquid) yield consistent sets of valence force constants, which reflect the trends in structural changes in this series. In the course of these normal-coordinate analyses it has been necessary to change some assignments found in the literature.

Introduction

The chlorofluorophosphoranes PCl_nF_{5-n} with n = 0–5 are the only complete series of phosphoranes with mixed ligands and are the most widely studied group. They have been scrutinized by various methods in the gas, liquid, and solid state and serve as useful model compounds for pentacoordinated derivatives. An excellent review of experimental and theoretical investigations of this series is given in ref 2. The basic structures of all members in this series have been established unambiguously by IR, Raman, NMR, and ^{35}Cl NQR spectroscopy. These methods confirm the predictions of the VSEPR theory,[3] i.e. trigonal-bipyramidal structures with the more electronegative fluorine atoms preferring axial positions (electronegativity or polarity rule[3,4]). Temperature-dependent ^{19}F NMR and vibrational studies give no evidence for the presence of any other isomeric forms.[2] An early visual analysis of electron diffraction intensities for PCl_2F_3[5] resulted in axial positions for the chlorine atoms (D_{3h} symmetry). This result has later been corrected by NMR[6,7] and vibrational spectroscopy[8] and by dielectric measurements, which demonstrate a nonzero dipole moment in the gas phase.[9]

Qualitative trends in bond lengths with increasing F/Cl substitution (i.e. with increasing n) have been predicted from variations of the stretching force constants[2,10–13] and from overlap populations derived from extended Hückel MO calculations.[14] The predicted variations in bond lengths, however, depend strongly on the method and assumptions used in deriving the force field and on the basis sets used in the theoretical calculations (with or without d functions). The angular distortions of the trigonal bipyramid can be predicted only qualitatively on the basis of the VSEPR model.[3] Although several structure determinations by gas electron diffraction have been reported for the extreme members of this series, PF_5[15–17] and PCl_5,[16,18,19] no studies have been performed for the mixed phosphoranes until very recently. In this paper we report electron diffraction results for the entire series PCl_nF_{5-n} with n = 1–4. Almost simultaneously with our studies, structure analyses for the two intermediate members, PCl_2F_3[20] and PCl_3F_2,[21] have been performed at Oregon State University.

In the course of our structure determinations, it became apparent that normal-coordinate analyses reported in the literature[2,10–13] do not result in consistent sets of force constants. Although experimental frequencies are reproduced very well in all cases, values for some parallel and perpendicular vibrational amplitudes calculated from these force fields are rather unrealistic. As an example, the force field for $PClF_4$[2] results in vibrational amplitudes $l(P–Cl_e)$ = 0.090 Å, $l(P–F_e)$ = 0.058 Å, and $l(P–F_a)$ = 0.044 Å as compared to experimental values of $l(P–Cl_e)$ = 0.056 (4) Å in PCl_5[19] and $l(P–F_e)$ = 0.041 (2) Å and $l(P–F_a)$ = 0.043 (2) Å in PF_5.[15] A vibrational reinvestigation for the chlorofluorophosphoranes is therefore included in this study, and valence force fields were determined for the entire series PCl_nF_{5-n} with n = 0–5.

Experimental Section

Preparation of Samples. All reactions were carried out in a Duran 50 glass vacuum line with nonlubricated stopcocks. Voltalef high-vacuum grease was used for all glass joints. The chlorofluorophosphoranes PCl_4F, PCl_3F_2, and PCl_2F_3 were prepared by the low-temperature chlorination reaction

$$PCl_nF_{3-n} + Cl_2 \rightarrow PCl_{2+n}F_{3-n} \quad (n = 0\text{–}2)$$

described by Holmes and Gallagher.[22] Pure chlorine gas was obtained by decomposition of $AuCl_3$. The samples were purified by repeated low-temperature vacuum fractionations.

Chlorotetrafluorophosphorane was prepared by the reaction of trichloroborane with pentafluorophosphorane

$$3PF_5 + BCl_3 \rightarrow 3PClF_4 + BF_3$$

by a procedure modified from that described by Neilson and Cowley.[23] The components were transferred under vacuum to a stainless-steel bulb, in order to suppress the formation of SiF_4. After 36 h at room temperature the reaction vessel was cooled to −100 °C, and the volatile products were separated by vacuum fractionation in a series of U-traps containing stainless-steel spirals. The traps were kept at −125, −155, and

---

(1) (a) Universität Tübingen. (b) Universität Dortmund.

(2) Holmes, R. R. *Pentacoordinated Phosphorus—I and II*; Monographs 175 and 176; American Chemical Society: Washington, DC, 1980; and references therein.

(3) Gillespie, R. J. *J. Am. Chem. Soc.* **1963**, *85*, 4671. Gillespie, R. J. *Molecular Geometry*; Van Nostrand Reinhold: London, 1972.

(4) Muetterties, E. L.; Mahler, W.; Schmutzler, R. *Inorg. Chem.* **1963**, *2*, 613.

(5) Brockway, L. O.; Beach, J. Y. *J. Am. Chem. Soc.* **1938**, *60*, 1836.

(6) Muetterties, E. L.; Mahler, W.; Pacher, K. J.; Schmutzler, R. *Inorg. Chem.* **1964**, *3*, 1298.

(7) Holmes, R. R.; Carter, R. P., Jr.; Peterson, G. E. *Inorg. Chem.* **1964**, *3*, 1748.

(8) Griffiths, J. E.; Carter, R. P., Jr.; Holmes, R. R. *J. Chem. Phys.* **1964**, *41*, 863.

(9) Holmes, R. R.; Carter, R. P. Jr.; *J. Chem. Phys.* **1965**, *43*, 1645.

(10) Holmes, R. R. *J. Chem. Phys.* **1967**, *46*, 3724.

(11) Holmes, R. R. *J. Chem. Phys.* **1967**, *46*, 3730.

(12) Beattie, I. R.; Livingston, K. M. S.; Reynolds, D. J. *J. Chem. Phys.* **1969**, *51*, 4269.

(13) Van Der Voorn, P. C.; Purcell, K. F.; Drago, R. S. *J. Chem. Phys.* **1965**, *43*, 3457.

(14) Van Der Voorn, P. C.; Drago, R. S. *J. Am. Chem. Soc.* **1966**, *88*, 3255.

(15) Hansen, K. W.; Bartell, L. S. *Inorg. Chem.* **1965**, *4*, 1775.

(16) Romanov, G. V.; Spiridonov, V. P. *J. Struct. Chem.* (*Engl. Transl.*) **1967**, *8*, 131.

(17) Spiridonov, V. P.; Ischenko, A. A.; Ivashkevich, L. S. *J. Mol. Struct.* **1981**, *72*, 153.

(18) Adams, W. J.; Bartell, L. S. *J. Mol. Struct.* **1971**, *8*, 23.

(19) McClelland, B. W.; Hedberg, L.; Hedberg, K. *J. Mol. Struct.* **1983**, *99*, 309.

(20) French, R. J.; Hedberg, K.; Shreeve, J. M.; Gupta, K. D. *Inorg. Chem.* **1985**, *24*, 2774.

(21) French, R. J.; Hedberg, K.; Shreeve, J. M. Paper presented at the Tenth Austin Symposium on Gas Phase Molecular Structure, 1984; TA 6.

(22) Holmes, R. R.; Gallagher, W. P. *Inorg. Chem.* **1963**, *2*, 433.

(23) Neilson, R. H.; Cowley, A. H. *Inorg. Chem.* **1975**, *14*, 2019.

0020-1669/86/1325-2828$01.50/0

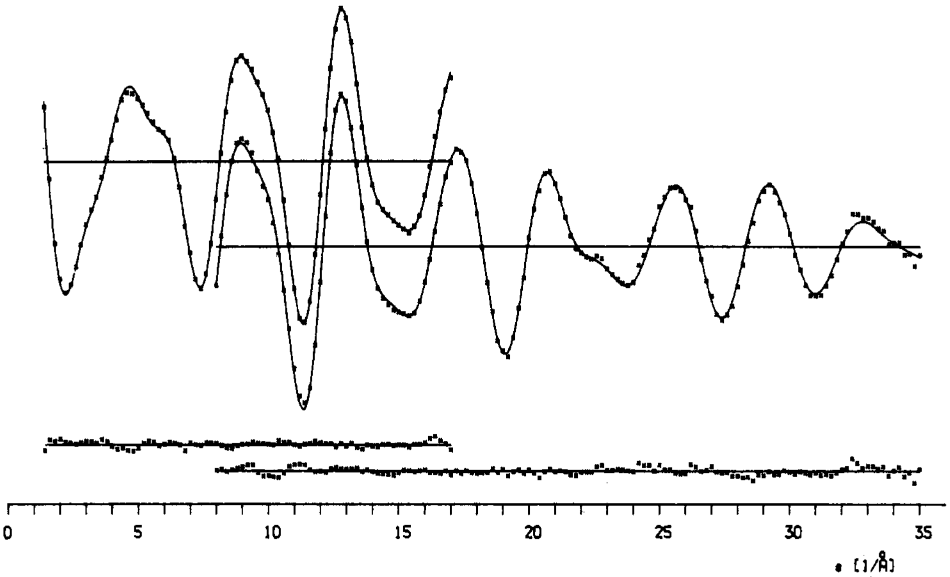

Figure 1. Experimental (···) and calculated (—) molecular intensities and differences for $PClF_4$.

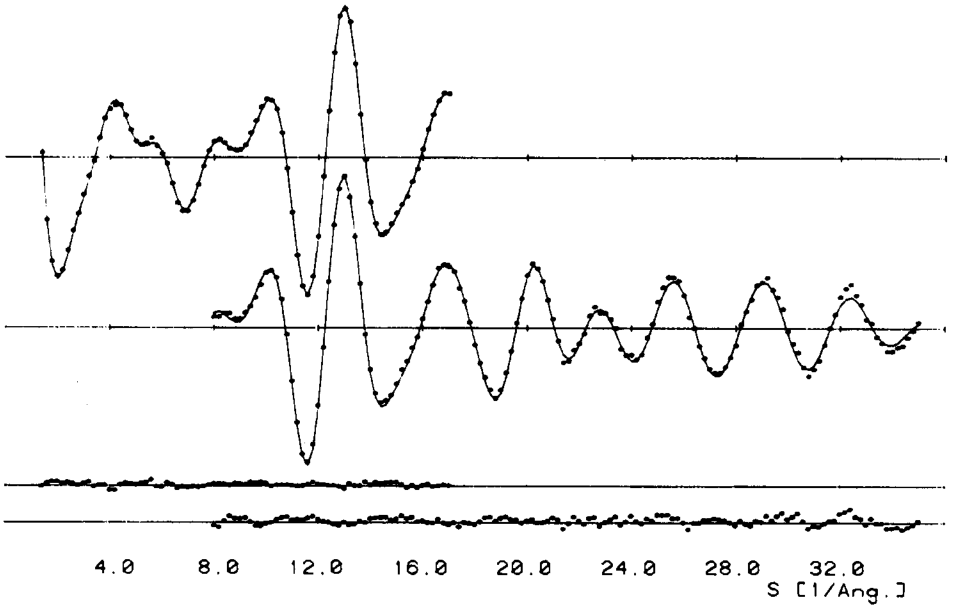

Figure 2. Experimental (···) and calculated (—) molecular intensities and differences for PCl_2F_3.

−196 °C. $PClF_4$ was retained at −155 °C together with small amounts of PF_5, which were removed by repeated low-temperature vacuum fractionations. In all cases the purity of the samples was checked by NMR, Raman, and matrix infrared spectra.

Vibrational Spectra. Matrix isolation spectra were obtained by condensation of the vapor above the samples mixed with an excess of argon on a cooled CsI window. The samples were kept at −145 °C ($PClF_4$), −130 °C (PCl_2F_3), −115 °C (PCl_3F_2), and −70 °C (PCl_4F). Deposition times were 30–60 min. The infrared spectra were recorded with a Perkin-Elmer 580 B instrument. The Raman spectra were measured with a Coderg T 800 spectrometer equipped with a Spectra Physics Ar^+ laser. The 488-nm line was used for excitation. The solid-state spectra were recorded at −196 °C, and polarization spectra at −100 °C ($PClF_4$), −78 °C (PCl_2F_3), −30 °C (PCl_3F_2), and room temperature (PCl_4F).

Electron Diffraction. The samples were transported in liquid nitrogen from Dortmund to Tübingen. The electron diffraction intensities were recorded with the Balzers Gasdiffractograph KD-G2[24] at two camera distances (25 and 50 cm) with an accelerating voltage of about 60 kV. The electron wavelength was calibrated by ZnO powder diffraction patterns, taken in every experiment. Additional calibration by CO_2 gas patterns in the experiments for $PClF_4$ and PCl_4F demonstrated that the ZnO and CO_2 values for the electron wavelength agreed within their standard deviations in these experiments (i.e., better than 0.05%). The samples were kept at −105 °C ($PClF_4$), −71 °C (PCl_2F_3), −45 °C (PCl_3F_2), and −4 °C (PCl_4F). The stainless-steel inlet system and nozzle were at room temperature in all experiments. The camera pressure never exceeded 1×10^{-5} torr. Exposure times were 5–9 s for the long camera distance and 20–45 s for the short distance. Two plates for each experiment were analyzed by the usual procedures.[25] Extraneous scattering

Table I. Fundamental Vibrations (cm^{-1}) of $PClF_4$[a]

no.	species (C_{2v})	IR (matrix)	Raman solid	Raman liquid	mode description
ν_1	a_1	889 vs	887 (19)	887 (7, p)	ν_s PF_2
ν_2		692 m	688 (100)	692 (100, p)	ν_s PF_2'
ν_3		557 s	551 (26)	560 (13, p)	δ PF_2'
ν_4		436 vw	445 (76)	438 (86, p)	ν PCl
ν_5			188 (16)	181 (9, p)	δ PF_2
ν_6	a_2		502 (8)	510 sh	τ PF_2F_2'
ν_7	b_1	989 vs	990 (5)	998 (1)	ν_{as} PF_2
ν_8		490 m	496 (12)	493 (9)	δ PF_2'
ν_9			145 (32)	144 (17)	δ $PClF_2$
ν_{10}	b_2	906 vs			ν_{as} PF_2'
ν_{11}		548 m			γ $PClF_2$
ν_{12}		357 vw	362 (18)	360 (8)	ρ $PClF_2F_2'$

[a] v = very, w = weak, m = medium, s = strong, sh = shoulder, p = polarized.

---

(24) Oberhammer, H. In *Molecular Structure by Diffraction Methods*; The Chemical Society: London, 1976; Vol. 4, p 234.

Table II. Fundamental Vibrations (cm^{-1}) of PCl_2F_3[a]

no.	species (C_{2v})	IR (matrix)	Raman solid	Raman liquid	mode description
ν_1	a_1	925 s	914 (4)	930 (3)	ν PF
ν_2		659 vs	659 (100)	652 (46, p)	ν_s PF_2'
ν_3		488 m	479 (30)	486 (17, p)	δ PF_2'
ν_4		410 vw	412 (73)	406 (100, p)	ν_s PCl_2
ν_5			128 (45)	123 (45, p)	δ PCl_2
ν_6	a_2		365 (16)	360 (8)	τ PCl_2F_2'
ν_7	b_1	647 s			ν_{as} PCl_2
ν_8		430 w	431 (16)	425 (13)	δ PF_2'
ν_9			165 (24)	172 (10)	δ PCl_2F
ν_{10}	b_2	884 s			ν_{as} PF_2'
ν_{11}		526 w	518 (2)		γ PCl_2F
ν_{12}		342 vw	342 (8)	340 (4)	ρ PCl_2FF_2'

[a] v = very; w = weak, m = medium, s = strong, p = polarized.

Table III. Fundamental Vibrations (cm^{-1}) of PCl_3F_2[a]

no.	species (D_{3h})	IR (matrix)	Raman solid	Raman liquid	mode description
ν_1	a_1		635 (51)	639 (38, p)	ν_s PF_2
ν_2			391 (100)	391 (100, p)	ν_s PCl_3
ν_3	a_2	859 s			ν_{as} PF_2
ν_4		330 vw			γ PCl_3
ν_5	e'	625 vs	625 (28)		ν_{as} PCl_3
ν_6		410 m	407 (40)	413 (9)	δ PF_2
ν_7			124 (78)	121 (80)	δ PCl_3
ν_8	e''		359 (24)	361 (7)	ρ PCl_3F_2

[a] v = very, w = weak, m = medium, s = strong, p = polarized.

Table IV. Fundamental Vibrations (cm^{-1}) of PCl_4F[a]

no.	species (C_{3v})	IR (matrix)	Raman solid	Raman liquid	mode description
ν_1	a_1	774 s			ν PF
ν_2		424 m	424 (100)	423 (100, p)	ν_s PCl_3
ν_3		339 m	333 (18)	335 (10, p)	ν PCl′
ν_4			306 (13)	305 (20, p)	γ PCl_3
ν_5	e	598 vs	597 (8)	594 (2)	ν_{as} PCl_3
ν_6		389 m	388 (5)	387 (7)	δ PCl′F
ν_7		264 vw	262 (15)	264 (11)	ρ $PCl_3Cl'F$
ν_8			110 (20)	110 (35)	δ PCl_3

[a] v = very, w = weak, m = medium, s = strong, p = polarized.

Table V. Force Constants (10^2 N/m) of PCl_nF_{5-n} (n = 0–5)

	PF_5	$PClF_4$	PCl_2F_3	PCl_3F_2	PCl_4F	PCl_5
$f(PF_e)$	6.467	6.229	6.057			
$f(PF_a)$	5.453	5.107	4.740	4.394	4.275	
$f(PCl_e)$		3.371	3.253	3.177	2.935	2.785
$f(PCl_a)$					2.184	1.959
$f(F_aPF_e)$	2.236	2.195	2.177			
$f(F_aPCl_e)$		1.920	1.862	1.830	1.841	
$f(Cl_aPCl_e)$					1.792	1.854
$f(F_ePF_e)$	0.284	0.266				
$f(F_ePCl_e)$		0.243	0.245			
$f(Cl_ePCl_e)$			0.232	0.232	0.206	0.168

recorded without gas was subtracted from the 25-cm data. The averaged molecular intensities over the ranges $1.4 < s < 17$ and $8 < s < 35$ Å^{-1} are shown in Figures 1–4 in steps of $\Delta s = 0.2$ Å^{-1}.

Vibrational Analysis

The infrared spectrum of matrix-isolated chlorotetrafluorophosphorane, $PClF_4$, is shown in Figure 5. The frequencies, states of polarization, and assignments are given in Table I. In the region of the PF-stretching fundamentals five bands appear in the infrared spectrum. In an earlier study[26] the vibration at 989 cm^{-1} was attributed to the hydrolysis product OPF_3. A matrix infrared spectrum of phosphoryl fluoride, recorded under similar conditions, clearly illustrates, however, that the 989-cm^{-1} band is due to the $PClF_4$ molecule. The band is assigned to the antisymmetric equatorial PF-stretching mode $\nu_7(b_1)$; the corresponding vibration in pentafluorophosphorane is observed at 1025 cm^{-1}.[2] The symmetric equatorial fundamental $\nu_1(a_1)$ is measured at 889 cm^{-1}, and the symmetric axial mode $\nu_2(a_1)$, also polarized in the liquid-state Raman spectrum, at 692 cm^{-1}. Two bands of similar intensities at 906 and 916 cm^{-1} are observed for the antisymmetric axial PF-stretching vibration $\nu_{10}(b_2)$ due to Fermi resonance with the combination $\nu_3(a_1) + \nu_{12}(b_2)$. The unperturbed ν_{10} vibration can be estimated from the intensity ratio[27] at 910 cm^{-1}. In the region of the axial bending modes three lines appear in the infrared spectrum, at 557, 548, and 490 cm^{-1}. An additional band at 502 cm^{-1} is observed in the low-temperature Raman spectrum. The axial PF_2-deformation mode $\nu_3(a_1)$ is assigned to the polarized Raman line at 560 cm^{-1}, and the corresponding $\nu_8(b_1)$ fundamental to the depolarized band at 493 cm^{-1}. The line at 502 cm^{-1}, which is observed only in the Raman spectra, is assigned to the infrared-inactive twisting mode $\nu_6(a_2)$, and the remaining vibration at 548 cm^{-1} to the out-of-plane fundamental $\nu_{11}(b_2)$. Two lines at low frequencies are observed in the Raman spectra, which are assigned to the equatorial in-plane-bend vibrations. The polarized band at 188 cm^{-1}, not observed by Holmes[26] because of a broad instrument ghost, is assigned to $\nu_5(a_1)$, and the depolarized band at 145 cm^{-1} to $\nu_9(b_1)$.

Dichlorotrifluorophosphorane, PCl_2F_3, has been studied by different authors;[2,8,12,20,28,29] the assignment of the fundamentals, however, is controversial. In the course of the normal-coordinate analysis it became apparent that the assignments of the symmetric equatorial and antisymmetric axial PF-stretching fundamentals $\nu_1(a_1)$ and $\nu_{10}(b_2)$ and the two in-plane-bending vibrations $\nu_5(a_1)$ and $\nu_9(b_1)$ have to be interchanged relative to ref 2, in order to obtain a set of force constants consistent with the other members of this series. The reassigned frequencies, relative intensities, and polarization data of PCl_2F_3 are summarized in Table II; the matrix infrared spectrum is shown in Figure 6.

The assignment of the vibrational frequencies of trichlorodifluorophosphorane, PCl_3F_2, (Table III) agrees with that published by Holmes.[2] The infrared spectrum of the matrix-isolated compound is presented in Figure 7.

Figure 8 shows the matrix infrared spectrum of tetrachlorofluorophosphorane. The Raman polarization study of PCl_4F leads to results different from those of an earlier investigation[8] and requires a reassignment especially of the deformation modes. The polarized lines in the liquid-state Raman spectrum at 335 and 305 cm^{-1} are attributed to the PCl-stretching fundamental $\nu_3(a_1)$ and to the out-of-plane mode $\nu_4(a_1)$, and the depolarized bands at 387 and 264 cm^{-1} to the axial PClF bending vibration $\nu_6(e)$ and to the rocking mode $\nu_7(e)$. The PF-stretching vibration $\nu_1(a_1)$ splits into a multiplet of bands in the infrared spectrum (774, 768, 760 sh, 756 cm^{-1}) due to a matrix site effect.[30] Annealing the matrix for a few seconds leads to a decrease of the 768- and 756-cm^{-1} lines and to an increase of the 774- and 760-cm^{-1} bands. A doublet of lines is also observed in an N_2 matrix. The splitting of ν_1 into two components is attributed to a Fermi resonance with the combination $\nu_2(a_1) + \nu_3(a_1)$. The unperturbed PF-stretching fundamental is estimated[27] at 771 cm^{-1}. Assignment of the other fundamentals is given in Table IV. The stretching fundamentals of the entire series PCl_nF_{5-n} (n = 0–5) are summarized in Figure 9.

Normal-Coordinate Analysis

Valence force fields of the phosphoranes PCl_nF_{5-n} with n = 0–5 were calculated with the programs NORKO[31] and NORCOR.[32] As far as possible, matrix infrared frequencies were used because of their greater accuracy. For PF_5 and PCl_5 the vibrational data given in ref 2 were used. For structural parameters, see Table VII. In the case of PF_5, the symmetry force field calculated by ab initio methods[33] was converted to a valence force field and the diagonal elements were adjusted to fit the experimental frequencies. Initial force fields for the mixed chlorofluorophosphoranes were based on this force field. The force constants for the entire series are summarized in Table V; interaction constants are not listed. The force fields reproduce the observed frequencies to within ±0.5 cm^{-1}. As expected, a decrease of the PF and PCl bond strengths occurs

---

(25) Oberhammer, H.; Gombler, W.; Willner, H. *J. Mol. Struct.* **1981**, *70*, 273.

(26) Holmes, R. R. *J. Chem. Phys.* **1967**, *46*, 3718.

(27) Saier, E. L.; Cousins, L. R.; Basila, M. R. *J. Phys. Chem.* **1962**, *66*, 232.

(28) Goubeau, J.; Baumgärtner, R.; Weiss, H. *Z. Anorg. Allg. Chem.* **1966**, *348*, 286.

(29) Salthouse, J. A.; Waddington, T. C. *Spectrochim. Acta, Part A* **1967**, *23A*, 1069.

(30) Barnes, A. J.; Orville-Thomas, W. J.; Müller, A.; Gaufrès, R. *Matrix Isolation Spectroscopy*; Reidel: Dordrecht, 1981.

(31) Bleckmann, P.; Schrader, B.; Meier, W.; Takahashi, H. *Ber. Bunsenges. Phys. Chem.* **1971**, *75*, 1279.

(32) Christen, D. *J. Mol. Struct.* **1978**, *48*, 101.

(33) Marsden, C. J. *J. Chem. Soc., Chem. Commun.* **1984**, 401.

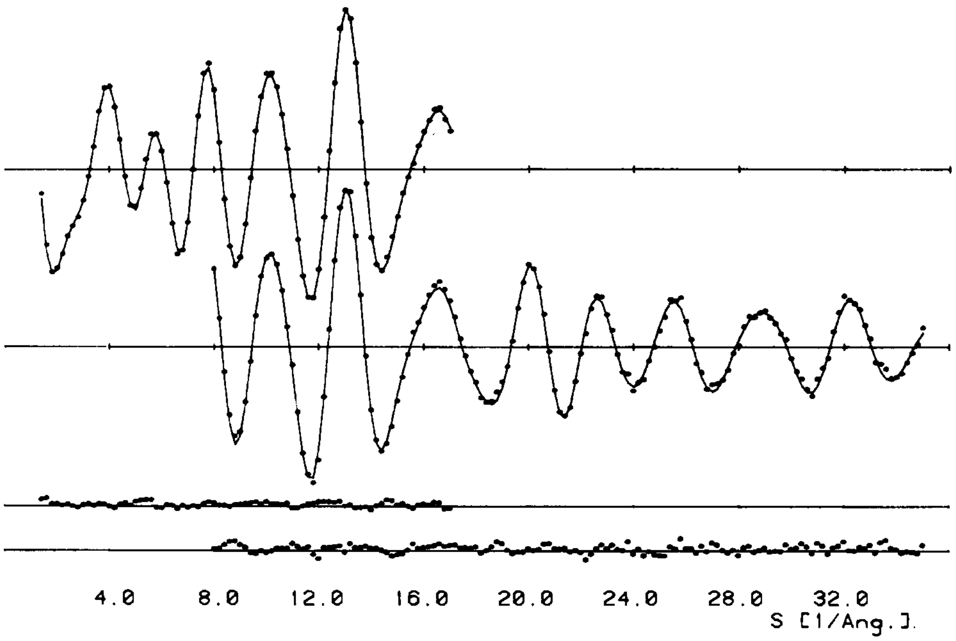

Figure 3. Experimental (···) and calculated (—) molecular intensities and differences for PCl_3F_2.

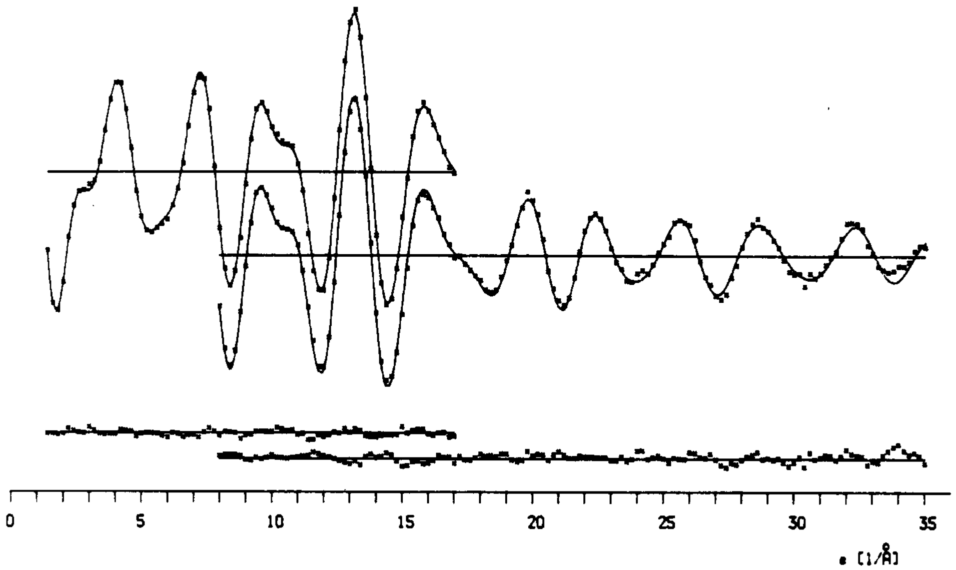

Figure 4. Experimental (···) and calculated (—) molecular intensities and differences for PCl_4F.

with increasing F/Cl substitution. Parallel to this a decrease of the bending force constants takes place. The large difference between axial and equatorial bending force constants is remarkable.

Structure Analysis

The radial distribution functions (Figures 10–13) were calculated from the molecular intensities with a damping constant $\gamma = 0.0019$ Å^2. For the region $s < 1.4$ Å^{-1} the theoretical intensities corresponding to the final model were taken. The geometric structures for the mixed chlorofluorophosphoranes are defined by five parameters if the symmetry is C_{2v} ($PClF_4$ and PCl_2F_3), by four parameters in the case of C_{3v} symmetry (PCl_4F), and by two bond lengths in PCl_3F_2 (D_{3h} symmetry). The number of "characteristic features" (peaks and shoulders) in the radial distribution curves is equal to or larger than the number of independent geometric parameters for all four compounds. As expected, the experimental radial distribution curves confirm the conformations that have been determined by various spectroscopic techniques (see the Introduction) and that conform with the electronegativity rule.

The geometric parameters in the r_α representation together with the vibrational amplitudes were refined in least-squares procedures. The harmonic vibrational corrections[34] $\Delta r = r_a - r_\alpha{}^0$ (see Table VI) were calculated from the force fields in Table V. For $PClF_4$ and PCl_2F_3 the ratio of axial and equatorial vibrational amplitudes was fixed to the spectroscopic value. No further constraints were required for the analyses. A diagonal weight matrix[25] was applied to the intensities and scattering amplitudes, and phases of Haase[35] were used. The following

Table VI. Harmonic Vibrational Corrections ($\Delta r = r_a - r_\alpha{}^0$) for PCl_nF_{5-n} (n = 1–4)

	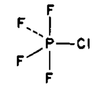	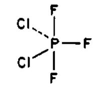	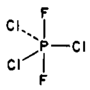	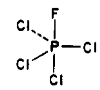
P–F_e	0.0031	0.0033		
P–F_a	0.0010	0.0011	0.0012	0.0016
P–Cl_e	0.0008	0.0019	0.0025	0.0030
P–Cl_a				0.0003
$F_e \cdots F_a$	0.0028	0.0016		
$F_e \cdots F_e$	0.0007			
$F_a \cdots F_a$	0.0000	0.0003	0.0005	
$Cl_e \cdots Cl_a$				0.0016
$Cl_e \cdots Cl_e$		–0.0025	–0.0017	–0.0016
$F_a \cdots Cl_e$	0.0008	0.0016	0.0022	0.0032
$F_e \cdots Cl_e$	–0.0019	–0.0007		
$F_a \cdots Cl_a$				0.0000

---

(34) Oberhammer, H. *J. Chem. Phys.* **1978**, *69*, 468.

(35) Haase, J. *Z. Naturforsch., A: Astrophys., Phys. Phys. Chem.* **1970**, *25A*, 936.

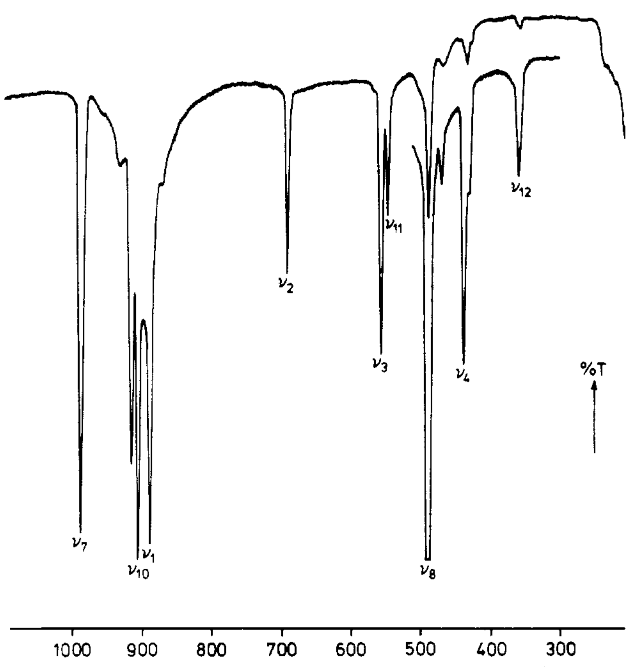

Figure 5. Infrared spectrum of matrix-isolated $PClF_4$.

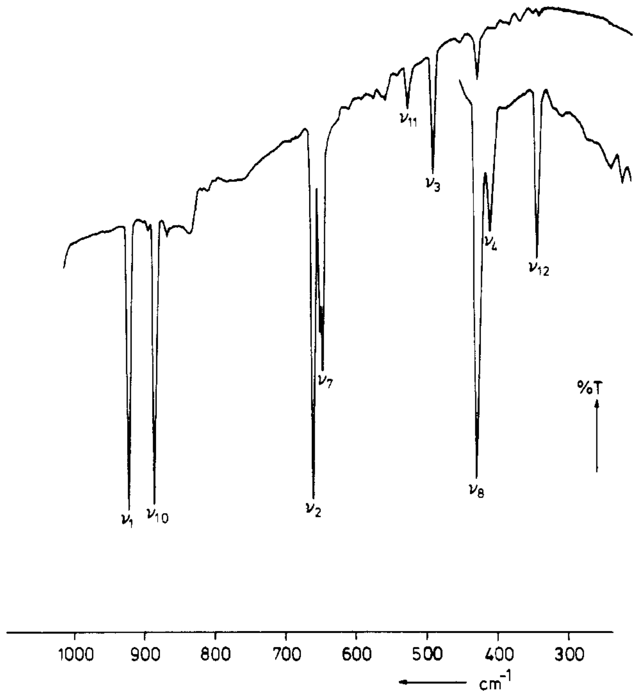

Figure 6. Infrared spectrum of matrix-isolated PCl_2F_3.

correlation coefficients had values larger than |0.6|.

$PClF_4$: $PF_e/PF_a = -0.92$, $PF_e/l(PF) = 0.83$, $PF_a/l(PF) = -0.92$, $F_ePF_e/l(F_a{\cdot}Cl_e) = -0.75$, $F_ePF_a/l(F_e{\cdot}F_e) = -0.65$.

PCl_2F_3: $PF_e/PF_a = -0.90$, $PF_a/F_ePF_a = -0.77$, $PF_a/F_ePF_a = 0.70$, $PF_e/l(PF) = 0.92$, $PF_a/l(PF) = -0.84$, $F_ePF_a/l(PF) = -0.70$.

PCl_4F: $PCl_e/PCl_a = 0.62$, $PCl_a/Cl_ePCl_a = 0.80$, $PCl_e/l(PCl_a) = 0.80$, $PCl_a/l(PCl_a) = 0.63$, $PCl_a/l(PCl_e) = -0.77$. No correlation larger than |0.6| occurred in the analysis for PCl_3F_2.

The final results for geometric parameters are summarized in Table VII. Bond lengths have been converted to r_g values. Error limits are 2σ values and include a possible scale error of 0.1% for bond lengths. Table VIII compares vibrational amplitudes from the electron diffraction experiment with those derived from the force fields. Error limits are here 3σ values. All geometric parameters and vibrational amplitudes for PCl_2F_3 and PCl_3F_2 derived in this study agree with the respective values obtained at Oregon State University within their combined error limits with only one exception: F_ePF_a in PCl_2F_3 is 90.0 (3)° in our study and 89.3 (3)° in the Oregon results.

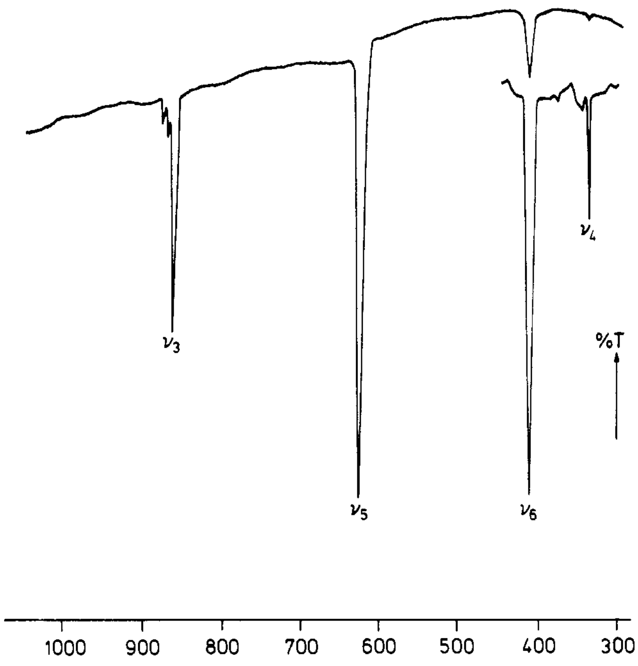

Figure 7. Infrared spectrum of matrix-isolated PCl_3F_2.

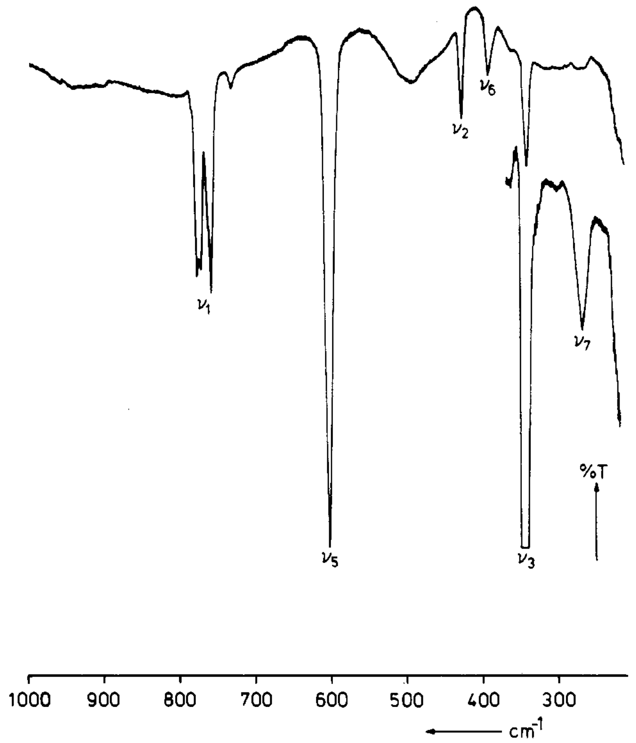

Figure 8. Infrared spectrum of matrix-isolated PCl_4F.

Results and Discussion

The equatorial and axial P–F and P–Cl bond lengths of the entire series of chlorofluorophosphoranes are shown in Figure 14 together with the corresponding stretching force constants. The perfect match in the trends of bond lengths and force constants together with the very good agreement between the vibrational amplitudes derived from electron diffraction and spectroscopic data (Table VIII) confirms the vibrational assignment of this study and the force fields.

Successive substitution of fluorine atoms in PF_5 by chlorine causes lengthening of all bonds, P–F and P–Cl, in equatorial and axial directions. The effects, however, are different for equatorial and axial bonds (see Figure 14). In general, the axial bonds are affected more strongly than equatorial bonds. The equatorial P–F

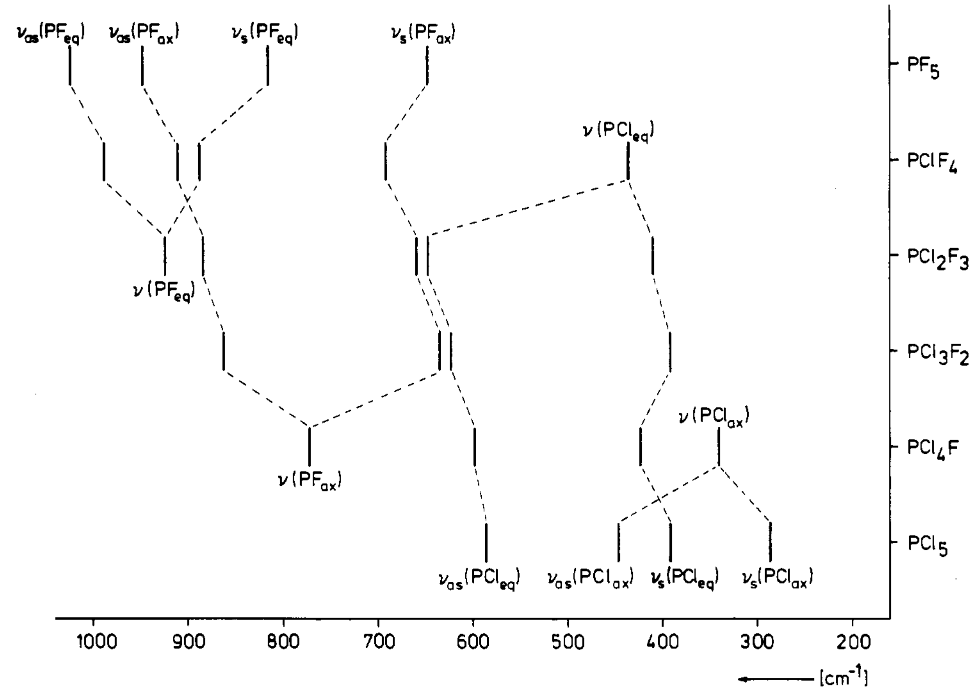

Figure 9. Stretching fundamentals (cm^{-1}) in the series PCl_nF_{5-n} (n = 0–5).

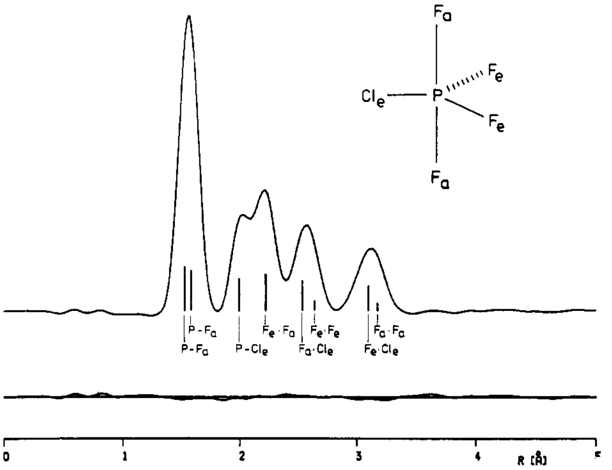

Figure 10. Experimental radial distribution function and difference curve for $PClF_4$.

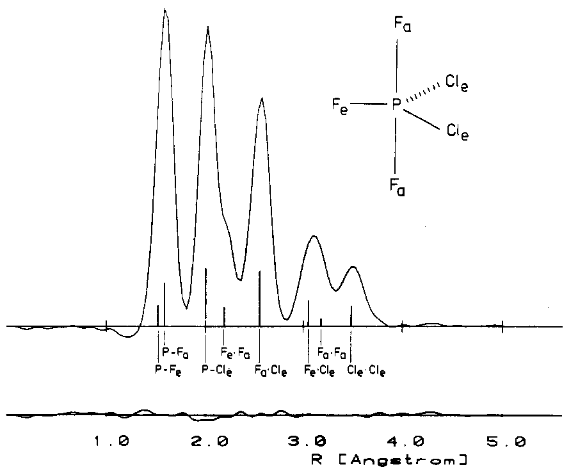

Figure 11. Experimental radial distribution function and difference curve for PCl_2F_3.

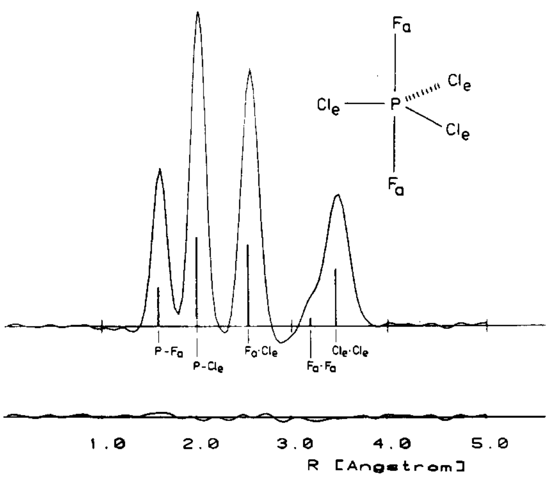

Figure 12. Experimental radial distribution function and difference curve for PCl_3F_2.

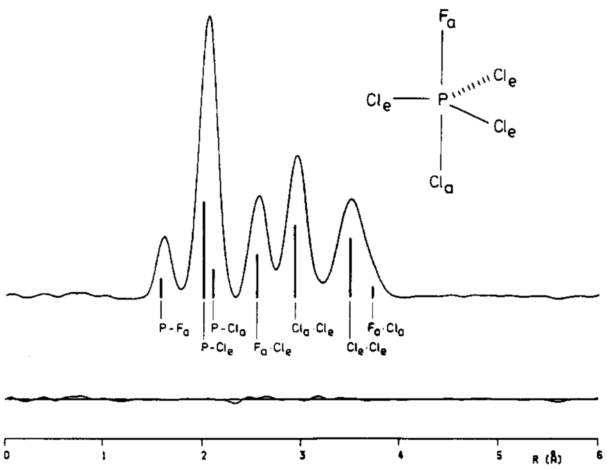

Figure 13. Experimental radial distribution function and difference curve for PCl_4F.

and P–Cl bonds lengthen only very little if *equatorial* fluorines are substituted by chlorines, i.e., for n = 0–3. (Within their experimental uncertainties these P–F_e and P–Cl_e bond lengths can be considered unaffected.) Substitution of *axial* fluorines by chlorine has a larger effect on the equatorial P–Cl bonds, i.e., for n = 4, 5. The axial P–F distances increase monotonically with

Table VII. Vibrational Amplitudes from Electron Diffraction (ed) and Spectroscopic Data (sp) for PCl_nF_{5-n} (n = 1–4)

	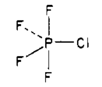		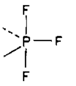		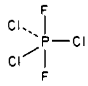		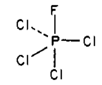	
	ed	sp	ed	sp	ed	sp	ed	sp
$P-F_e$	0.043 (5)[a]	0.040	0.044 (6)[a]	0.040				
$P-F_a$	0.046 (5)[a]	0.043	0.048 (6)[a]	0.043	0.042 (3)	0.044	0.040 (7)	0.044
$P-Cl_e$	0.053 (3)	0.046	0.051 (3)	0.046	0.046 (2)	0.046	0.049 (3)	0.048
$P-Cl_a$							0.057 (9)	0.055
$Fe\cdots F_a$	0.061 (3)	0.060	0.055 (5)	0.060				
$F_e\cdots F_e$	0.072 (19)	0.085						
$F_a\cdots F_a$	0.064 (16)	0.053	0.073 (21)	0.054	0.039 (19)	0.055		
$Cl_e\cdots Cl_a$							0.078 (3)	0.073
$Cl_e\cdots Cl_e$			0.107 (9)	0.104	0.102 (4)	0.105	0.110 (5)	0.111
$F_a\cdots Cl_e$	0.079 (6)	0.065	0.077 (4)	0.066	0.067 (2)	0.066	0.063 (4)	0.067
$F_e\cdots Cl_e$	0.109 (8)	0.095	0.104 (9)	0.094				
$F_a\cdots Cl_a$							0.078 (21)	0.063

[a] Ratio of $(P-F_e)/(P-F_a)$ was constrained to spectroscopic value.

Table VIII. Geometric Parameters (r_g Distances and r_α Angles) for PCl_nF_{5-n} (n = 0–5)

	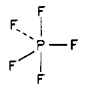	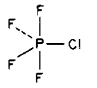	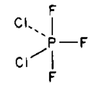	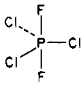	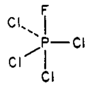	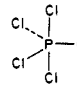
$P-F_e$	1.534 (4)	1.535 (3)	1.538 (7)			
$P-F_a$	1.577 (5)	1.581 (4)	1.593 (4)	1.596 (2)	1.597 (4)	
$P-Cl_e$		2.000 (3)	2.002 (3)	2.005 (3)	2.011 (3)	2.023 (3)
$P-Cl_a$					2.107 (6)	2.127 (3)
X_ePX_e	120[a]	117.8 (7)[a]	121.8 (4)[b]	120[b]	120.0 (1)[b]	120[b]
X_ePY_a	90[c]	90.3 (4)[c]	90.0 (3)[c]	90[d]	90.9 (2)[e]	90[e]

[a] F_ePF_e. [b] Cl_ePCl_e. [c] F_ePF_a. [d] Cl_ePF_a. [e] Cl_ePCl_a.

successive replacement of *equatorial* fluorines by chlorine (n = 0–3), but within experimental uncertainties $P-F_a$ is not affected if the remaining *axial* fluorine is exchanged. The largest substitution effect within this series is observed for the axial P–Cl bond if the opposite axial fluorine is substituted, i.e., between PCl_4F and PCl_5.

The angular distortions of the trigonal bipyramids are surprisingly small. The equatorial bond angles in $PClF_4$ (F_ePF_e = 117.8 (7)°) and in PCl_2F_3 (Cl_ePCl_e = 121.8 (4)°) deviate only by about 2° from the ideal 120°, and the direction of these deviations agrees with the prediction of the VSEPR model (F_ePF_e < 120° and Cl_ePCl_e > 120°). The deviations of the equatorial–axial bond angles are even smaller, as expected from the much larger force constants for these angle bendings. They are less than 1° in all cases. In $PClF_4$ and PCl_2F_3 these distortions of the F_ePF_a angles (90.3 (4) and 90.0 (3)°, respectively) are less than the experimental uncertainties. For $PClF_4$ the direction of the distortion (F_ePF_a > 90°) appears to contradict the prediction of the VSEPR model (F_ePF_a < 90°), but the uncertainty in the distortion is larger than the value itself. Only in PCl_4F is the distortion of the axial–equatorial angle (Cl_ePCl_a = 90.9 (2)°) larger than the experimental uncertainty.

Bonding in pentacoordinated phosphorus compounds has attracted considerable interest during the past decades by experimentalists and theoreticians (see ref 2 and 36 and references therein). Essentially, three different bonding models have been proposed: (1) an electron-deficient model with sp^2 hybrids in equatorial directions and three-center four-electron bonds in axial directions;[37] (2) directed valence with participation of phosphorus 3d orbitals forming pd hybrids in axial directions;[38] (3) VSEPR theory.[3] All three models predict the axial bonds to be longer than the equatorial bonds and a general lengthening of all bonds in the chlorofluorophosphorane series with increasing F/Cl substitution. In the MO picture, the valence orbitals expand with decreasing number of fluorine substituents and the polar contributions decrease in the same direction. In the VSEPR picture the repulsions between the bonding electron pairs increase if fluorine is replaced by chlorine, and this leads to bond lengthening. Overlap populations derived from extended Hückel MO calculations for the PCl_nF_{5-n} series decrease for all bonds with increasing n. If phosphorus 3d functions are included in the basis set, these calculations predict nearly equal lengthening of axial and equatorial bonds, whereas calculations without d functions predict stronger lenghthening of axial relative to equatorial bonds. These

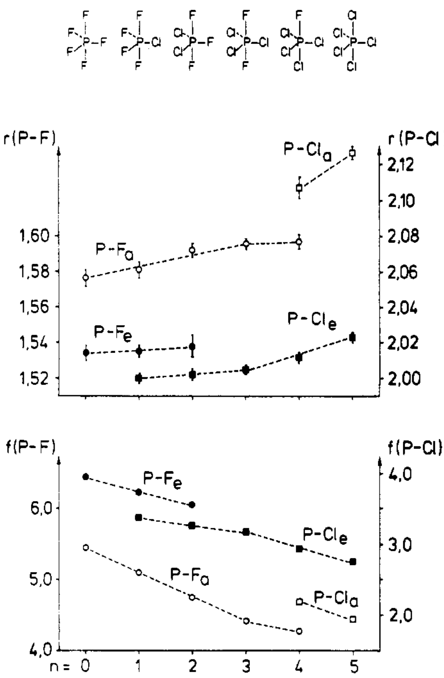

Figure 14. Equatorial and axial P–F and P–Cl bond lengths (above) and corresponding force constants (below) for the series PCl_nF_{5-n}, n = 0–5).

---

(36) Mc Dowell, R. S.; Streitwieser, A., Jr. *J. Am. Chem. Soc.* **1985**, *107*, 5849.

(37) Rundle, R. E. *Rec. Chem. Prog.* **1962**, *23*, 195.

(38) Craig, D. P.; Maccoll, A.; Nyholm, R. S.; Orgel, L. E.; Sutton, L. E. *J. Chem. Soc.* **1954**, 332.

latter calculations which correspond closely to the electron-deficient model, reproduce the experimental trends much better than the calculations with d functions. The actual bonding situation in these phosphoranes is intermediate between models 1 and 2. Ab initio calculations for PF_5 report populations of d functions between 0.64[39] and 1.13 au.[40] Furthermore, polar contributions to both axial and equatorial bonds have to be considered.

Acknowledgment. H.O. and B.S. gratefully acknowledge financial support by the Deutsche Forschungsgemeinschaft.

Registry No. $PClF_4$, 13637-88-2; PCl_2F_3, 13454-99-4; PCl_3F_2, 13537-23-0; PCl_4F, 13498-11-8.

---

(39) Strich, A.; Veillard, A. J. *J. Am. Chem. Soc.* **1973**, *95*, 5574.

(40) Howell, J. M.; Van Wazer, J. R.; Rossi, A. R. *Inorg. Chem.* **1974**, *13*, 1747.

Contribution from the Department of Chemistry and Program in Biochemistry and Biophysics,
Washington State University, Pullman, Washington 99164-4630

Solution Structure of $[Cr^{III}(L)(O\text{-}O)]^n$ Complexes (L = Nitrilotriacetate, *N*,*N*-β-Alaninediacetate; O-O = Malonate, Oxalate, Acetylacetonate, $2H_2O$) and Characterization of $[Cr(nta)(OH)]_2^{2-}$ by Deuteron NMR Spectroscopy

Norio Koine,[1] Robert J. Bianchini, and J. Ivan Legg*

Received July 31, 1985

The complexes $[Cr^{III}(L)(O\text{-}O)]^n$ (L = nitrilotriacetate (nta), *N*,*N*-β-alaninediacetate (β-alada); O-O = malonate (mal), oxalate (ox), acetylacetonate (acac), $2H_2O$) have been synthesized, chromatographically purified, and characterized by deuteron NMR, infrared and electronic absorption spectroscopy. The two possible isomers, symmetrical (sym) and unsymmetrical (unsym), for $[Cr(\beta\text{-alada})(acac)]^-$ and $[Cr(\beta\text{-alada})(mal)]^{2-}$ were isolated, but only the unsym isomer for $[Cr(\beta\text{-alada})(ox)]^{2-}$ was found. The starting materials for the synthesis of these complexes, $[Cr(nta)(OH)]_2^{2-}$ and *unsym*-$[Cr(\beta\text{-alada})(H_2O)_2]$, were also characterized. Both species were shown to be in equilibrium with the corresponding monomer and dimer, respectively. The chemistry of the various species investigated differs, to some extent, from what has been previously reported. The recent availability of a readily applicable NMR technique for the study of Cr(III) chemistry (^2H NMR) has greatly facilitated these studies.

Introduction

Numerous studies of the aminetricarboxylate ligand ($N(-O)_3$) complexes of the substitution-inert metal ions chromium(III)[2–7] and cobalt(III)[2,8–10] have been reported. When these tripodlike ligands function as quadridentate chelating agents, two cis sites remain (Figure 1). Complexes such as these, where the two remaining sites are occupied by water molecules, exhibit a propensity to dimerize in aqueous solution to give bis(μ-hydroxo)-bridged species.[8,11–18] The Co(III) complex of the tripodlike ligand nitrilotriacetate (nta)[19] readily forms a bis(μ-hydroxy)-bridged dimer.[8] Absorption spectral studies of Cr(III) complexes of these two ligands as well as of another nta analogue, *N*,*N*-β-alaninediacetate (β-alada), have concluded that $N(-O)_3$ ligands can function both as quadridentate and terdentate (three acetates coordinated) chelating agents, but dimer formation was not reported.[2,5–7]

The studies of Co(III)–nta complexes were facilitated significantly by ^1H NMR spectroscopy.[20] Unfortunately, until recently it has not been possible to do structural studies on Cr(III) complexes by NMR due to the extreme line broadening of resonances brought about by the long electron spin relaxation times associated with paramagnetic Cr(III). Recently we have demonstrated that ^2H NMR can be used to study the solution chemistry of Cr(III) complexes.[21–23] Since $N(-O)_3$ ligands can be prepared readily

---

(1) On leave from Eihme University, Ehime, Japan.

(2) Uehara, A.; Kyuno, E.; Tsuchiya, R. *Bull. Chem. Soc. Jpn.* **1970**, *43*, 414.

(3) Fujii, Y.; Kyuno, E.; Tsuchiya, R. *Bull. Chem. Soc. Jpn.* **1969**, *42*, 1301.

(4) Uehara, A.; Kyuno, E.; Ryokichi, T. *Bull. Chem. Soc. Jpn.* **1968**, *41*, 2393.

(5) Uehara, A.; Kyuno, E.; Tsuchiya, R. *Bull. Chem. Soc. Jpn.* **1968**, *41*, 2385.

(6) Uehara, A.; Kyuno, E.; Tsuchiya, R. *Bull. Chem. Soc. Jpn.* **1967**, *40*, 2322.

(7) Uehara, A.; Kyuno, E.; Tsuchiya, R. *Bull. Chem. Soc. Jpn.* **1967**, *40*, 2317. Tsuchiya, R.; Uehara, A.; Kyuno, E. *Bull. Chem. Soc. Jpn.* **1969**, *42*, 1886.

(8) (a) Meloon, D. R.; Harris, G. M. *Inorg. Chem.* **1977**, *16*, 434. (b) Mori, M.; Shibata, M.; Kyuno, E.; Okubo, Y. *Bull. Chem. Soc. Jpn.* **1958**, *31*, 437.

(9) Koine, N.; Sakota, N.; Hidaka, J.; Shimura, Y. *Inorg. Chem.* **1973**, *12*, 859.

(10) Koine, N.; Sakota, N.; Hidaka, J.; Shimura, Y. *Bull. Chem. Soc. Jpn.* **1969**, *42*, 1583.

(11) Ardon, M.; Bino, A. *Inorg. Chem.* **1984**, *24*, 1343.

(12) Ranger, G.; Beauchamp, A. L. *Acta Crystallogr., Sect. B: Struct. Crystallogr. Cryst. Chem.* **1981**, *B37*, 1063.

(13) Srdanov, G.; Herak, R.; Radanović, D. L.; Vesselinović, D. S. *Inorg. Chim. Acta* **1980**, *38*, 37.

(14) Toftlund, H.; Springborg, J. *J. Chem. Soc., Chem. Commun.* **1976**, 1017.

(15) Springborg, J.; Toftlund, H. *Acta Chem. Scand., Ser. A* **1976**, *A30*, 171. Kaas, K. *Acta Crystallogr., Sect. B: Struct. Crystallogr., Cryst. Chem.* **1979**, *B35*, 1603. Christensson, F.; Springborg, J. *Acta Chem. Scand., Ser. A* **1982**, *A36*, 21.

(16) Kaas, K. *Acta Crystallogr., Sect. B: Struct. Crystallogr., Cryst. Chem.* **1976**, *B32*, 202.

(17) El-Awady, A. A.; Hugus, Z. Z., Jr. *Inorg. Chem.* **1971**, *10*, 1415.

(18) Grant, D. M.; Hamm, R. E. *J. Am. Chem. Soc.* **1958**, *80*, 4166.

(19) Abbreviations: nta = nitrilotriacetate; β-alada = *N*,*N*-β-alaninediacetate; acac = acetylacetone (1,3-pentanedione); mal = malonate; ox = oxalate; gly = glycinate.

(20) Smith, B. B.; Sawyer, D. T. *Inorg. Chem.* **1968**, *7*, 922.

(21) Bianchini, R. J.; Geiser, U.; Place, H.; Kaisaki, S.; Morita, Y.; Legg, J. I. *Inorg. Chem.*, in press.

(22) Bianchini, R. J.; Legg, J. I., in press. Broderick, W. E.; Legg, J. I. *Inorg. Chem.* **1985**, *24*, 3724. Wheeler, W. D.; Legg, J. I. *Inorg. Chem.* **1985**, *24*, 1292. Wheeler, W. D.; Legg, J. I. *Inorg. Chem.* **1984**, *23*, 3798. Green, C. A.; Bianchini, R. J.; Legg, J. I. *Inorg. Chem.* **1984**, *23*, 2713.

(23) Wheeler, W. D.; Kaizaki, S.; Legg, J. I. *Inorg. Chem.* **1982**, *21*, 3248.